Chapter 6
Speciation in Shock Tubes

Kenji Yasunaga and Robert S. Tranter

Abstract A shock tube is a device in which a shock wave is normally formed by the rupture of a diaphragm, which divides a gas at high pressure from a test section containing the species of interest at a lower pressure. The shock wave brings the test gas virtually instantaneously to a known high temperature and pressure, maintains that condition for a time and then is supplanted by an expansion wave which cools the sample rapidly. During this time, the test gas can be studied by continuous sampling, for example to a time-of-flight mass spectrometer or alternatively sampled at the end of process by gas chromatography or other appropriate analytical techniques. Here, we discuss both methodologies and show with examples the benefits of both approaches.

6.1 Introduction

Complex phenomena such as ignition delay times and laminar flame speeds are useful measures of the reactivities of fossil or bio-fuels and are therefore widely used for the validation of detailed chemical kinetic models (Simmie 2003). However, measurements of the reactants, intermediates and products formed during a pyrolytic or combustion event are much more valuable since they provide direct evidence of the chemical changes taking place. Thus, 'speciation' is the subject of this chapter, and it will deal with two different approaches to this end.

K. Yasunaga (✉)
Department of Applied Chemistry, National Defense Academy, 1-10-20 Hashirimizu, Yokosuka, Japan
e-mail: yasunaga@nda.ac.jp

R. S. Tranter (✉)
Chemical Sciences and Engineering, Argonne National Laboratory, 9700 S. Cass Ave. Argonne, Argonne, IL 60439, USA
e-mail: Tranter@anl.gov

F. Battin-Leclerc et al. (eds.), *Cleaner Combustion*, Green Energy and Technology,
DOI: 10.1007/978-1-4471-5307-8_6,

One can categorize shock tubes into two distinct classes; the first a single pulse shock tube can produce speciation data at the end of shock heating whilst the second, more conventional type, can produce time dependent speciation. Time-dependent speciation can be obtained by coupling the shock tube to a mass spectrometer, typically a time-of-flight, which can separate and quantify ions at a high repetition rate. Nonintrusive optical diagnostics are also employed but are not able to identify and quantify more than a few species at this moment of time and are not considered here. However, considerable progress is being made on multispecies optical diagnostics (Davidson et al. 2011).

6.2 Single Pulse Shock Tube

Single pulse shock tubes are designed to heat a gas mixture for a constant period, the dwell or residence time, at a high temperature, the reflected shock temperature, and then rapidly quench the hot gases back to room temperature preserving the high temperature composition. The resulting gases are then sampled and analyzed.

This combination of single pulse shock tubes and gas sampling has been used to investigate a large number of species some illustrative examples of which include halogen compounds (Simmie et al. 1969; Tsang and Lifshitz 1999; Rajakumar et al. 2002), oxygenates (Herzler et al. 1997; Lifshitz and Ben Hamou 1983; Hidaka et al. 1989) and aromatic hydrocarbons (Lifshitz et al. 2004; Sivaramakrishnan et al. 2006). In each experiment profiles of species concentrations with respect to temperature and pressure are obtained. Often kinetic data can be extracted and frequently the data are used to also develop and validate complex mechanisms. For instance, species profiles obtained for oxygenates (Yasunaga et al. 2010, 2012) are being utilized to validate detailed chemical kinetic mechanisms. Some of the species encountered have very low vapor pressures which renders sampling problematic because of condensation and subsequent loss of sample. So heating systems for the mixture preparation section, the manifold, the shock tube itself and the sampling system have been constructed to circumvent this problem for single pulse shock tubes (Lifshitz et al. 2009).

Single pulse shock tubes are currently operating that collectively span an enormous range of reaction pressures from subatmospheric to 1,000 bar. Typically, the shock tubes are operated with reaction temperatures <2,500 K with the upper limit being defined by rate of reaction and the residence time, typically 1–3 ms, which is a function of the shock tube geometry. The analytical techniques, primarily gas chromatography, used in single pulse shock tube work are generally very sensitive and the initial concentration of reagents introduced into the shock tube normally fall in the range 10 ppm to 1 % with concentrations in the 50–200 ppm range being the norm.

6.2.1 Principle of Single Pulse Shock Tube

The single pulse shock tube commonly used is a magic-hole-type shock tube (Hidaka et al. 1985; Lifshitz et al. 1963). These tubes are composed of high- and low-pressure sections and a dump tank. The function of the dump tank is to 'swallow' the reflected shock wave and prevent multiple re-heating of the test gases.

A schematic diagram of a single pulse shock tube is shown in Fig. 6.1. Operation of a single pulse shock tube involves filling the low pressure section and dump tank to the same pressure, pressurizing the high pressure section and bursting the diaphragm. Sample gas is collected through a sampling port after shock heating for analysis. Two methods are commonly used. In the first method, gases are simply withdrawn through an orifice located in the center of the end wall of the driven section. In the second method, a gas collection pipe is pushed through a port in the sidewall of the driven section near the endwall to the center of the shock tube before collection of a sample begins. This later design has been chosen to avoid collecting test gas from the side wall boundary layer that forms behind the shock wave because this has not experienced the full temperature behind the reflected shock and consequently has not undergone the same chemical change as the bulk gas mixture itself. A typical side wall sample port is shown in Fig. 6.2.

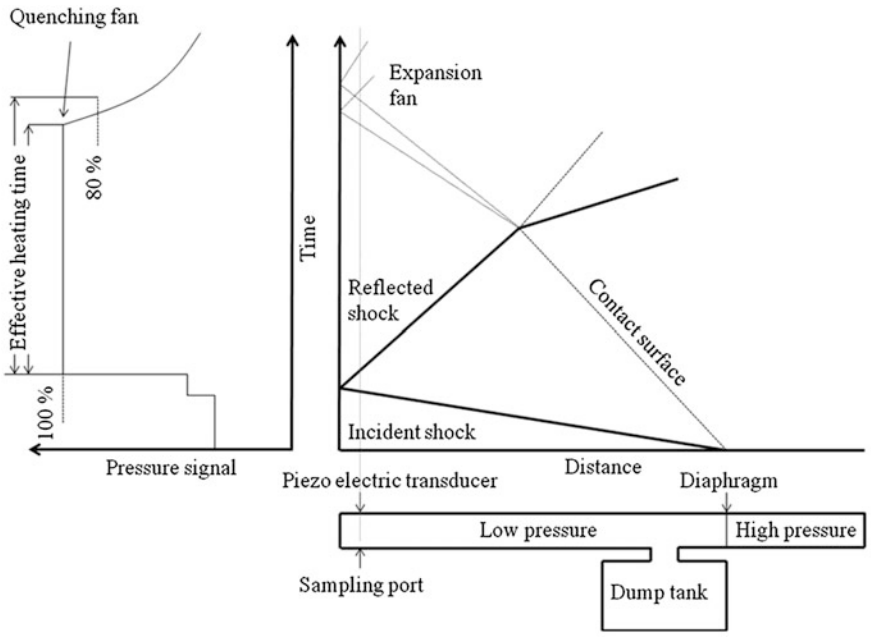

Fig. 6.1 Schematic diagram of single-pulse shock tube

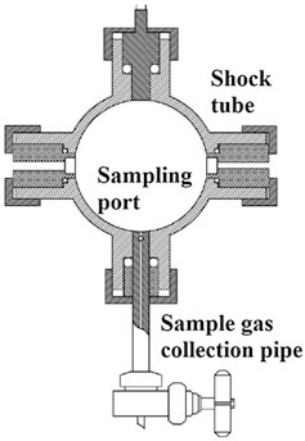

Fig. 6.2 Schematic diagram of sample port

The temperature behind the incident shock wave is commonly very low, and the timescale is insufficient to activate the chemical reaction compared to that behind the reflected shock wave, so the sample gas is effectively heated just once. Pressure remains constant for a certain period after the arrival of the reflected shock wave, and then the pressure rapidly decreases due to the arrival of the quenching fan. A typical pressure trace is shown in Fig. 6.3.

From the equation of adiabatic expansion which relates the pressure, p, at time t and the reflected shock pressure p_5 to the reflected shock temperature T_5 and the temperature T during the cooling phase we have:

$$p/p_5 = (T/T_5)^{\{\gamma/(\gamma-1)\}}$$

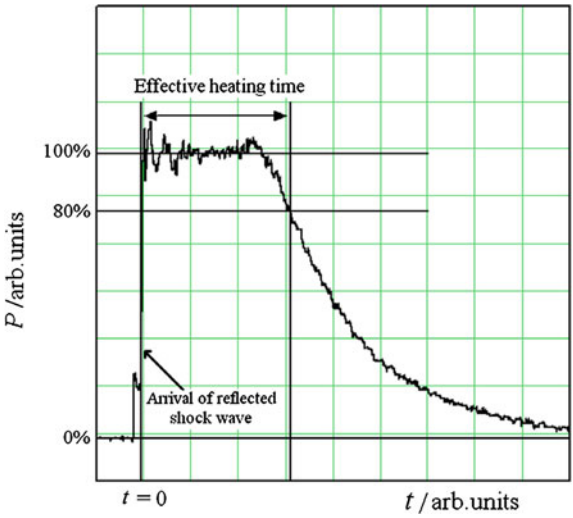

Fig. 6.3 A typical pressure profile with the definition of effective heating time

And the rate of change of temperature is described by:

$$(\mathrm{d}T/\mathrm{d}t) = \{(\gamma - 1)/\gamma\}(T_5/p_5)(\mathrm{d}p/\mathrm{d}t)$$

where γ is ratio of specific heats after shock heating behind the reflected shock wave. The cooling rate can therefore be estimated from the slope of pressure versus time. Typical cooling rates of 10^5–10^6 K s^{-1} reported (Lifshitz et al. 1963; Hidaka et al. 1985) are so large that the chemical reactions are frozen very quickly; however, some reactions do persist during this cooling phase. In order to account for this we define here an effective reaction time as the time interval between shock wave arrival at the end-plate and until such time as the reflected shock pressure has decreased to 80 % of its maximum value, Fig. 6.3.

6.2.2 Data Acquisition

Most single pulse shock tubes are coupled to one or more gas chromatographs to determine the concentrations of reactants and products as a result of shock heating. However, sometimes samples are withdrawn into sample vessels for later analysis or to utilize analytical instruments at a different facility. A variety of detectors such as thermal conductivity, flame ionization, electron capture, mass spectrometric, and others can be mounted on the gas chromatographs allowing most organic species to be detected.

The calibration methods to estimate the concentrations of reactant and products are introduced below. The sensitivities of the detector to each species is determined by developing calibration curves of the detector response, peak area (or height), to known concentrations of the species. These sensitivities are normalized against standard species which helps minimize error in calibration. Possible candidates for standard species include the diluent gases, usually argon or nitrogen. The merit of this method is that it does not require a perfect mass balance. However, this method is restricted to the case in which the diluent gases are capable of being detected. One of the authors commonly uses a gas chromatograph with a TCD, which can detect reactants, products and argon. Similar techniques can be employed with other detectors, which are not sensitive to inert gases by selecting appropriate standard molecules. The sensitivity, *S,* against argon as an internal standard is calculated for species X in a series of calibration experiments in which measured area ratios are related to known concentration ratios as:

$$S = (A_X/A_{Ar}) \times ([Ar]/[X])$$

where A is the peak area and the square brackets denote concentration. The concentrations of species, [X], as a result of shock heating are estimated using the sensitivity together with measured area ratios and the known concentration of argon:

$$[\mathrm{X}] = (1/S) \times (A_{\mathrm{X}}/A_{\mathrm{Ar}}) \times [\mathrm{Ar}]$$

Typically, a 95–105 % mass balance of chemical species is obtained using this method provided that the sample is not adsorbed or condensed or polymerizes during the transfer process.

6.2.3 Validation of Single Pulse Shock Tube

The data produced by a single pulse shock tube experiment are a little unusual in that one obtains a distribution of species concentrations after some reaction time at a particular temperature and pressure. Due to a number of constraints, it is difficult to vary the reaction time. Thus, an experimental dataset consists of points spanning a wide range of temperature, a small range of reaction times and a small pressure range. For a simple unimolecular reaction, it is possible to recover accurate rate coefficients from these data by simulating each experiment. For more complex reactions, it is still be possible to recover kinetic data although the datasets may be more useful as targets for model development. To validate the single pulse shock tube technique and show that reliable kinetic data can be obtained Tsang and Lifshitz (2001) compared the results of single pulse shock tube experiments with those from other reactors. For the validation, they selected a series of unimolecular decomposition reactions, which include direct formation of stable products to reduce the complexity of chemical reactions.

Ethyl *tert*-butyl ether (ETBE) is a good example of a suitable validation molecule because it decomposes mainly via a molecular elimination reaction under single pulse shock tube conditions:

$$(\mathrm{CH_3})_3\mathrm{COC_2H_5} = (\mathrm{CH_3})_2\mathrm{C} = \mathrm{CH_2} + \mathrm{C_2H_5OH} \qquad (6.1)$$

producing stable species directly. The kinetics of this process was measured by Yasunaga et al. (2008) using both a single pulse shock tube coupled to a GC and a conventional shock tube with UV absorption spectroscopy. The results of single pulse shock tube experiments are shown in Fig. 6.4 together with a computer simulation. The rate constant of 1.7×10^{14} exp(−254,000 J mol^{-1}/*RT*) s^{-1} for reaction (6.1) was estimated to explain the decomposition of ETBE and production of isobutene and ethanol.

The rate of reaction (6.1) was also estimated by monitoring the time-dependent concentration of isobutene and ETBE at high dilution to reduce the influence of secondary reactions. A typical absorbance profile for ETBE decomposition with simulation lines at 195 nm is shown in Fig. 6.5. The main absorbers at 195 nm in the ETBE pyrolysis system are ETBE and isobutene. After the arrival of the reflected shock wave, the absorbance profile shows rapid increases due to the absorption by ETBE, then gradually grows because isobutene is produced through the reaction (6.1). The influence of secondary reactions is so small that absorbance profiles can be approximately reproduced using simple first order equations, as

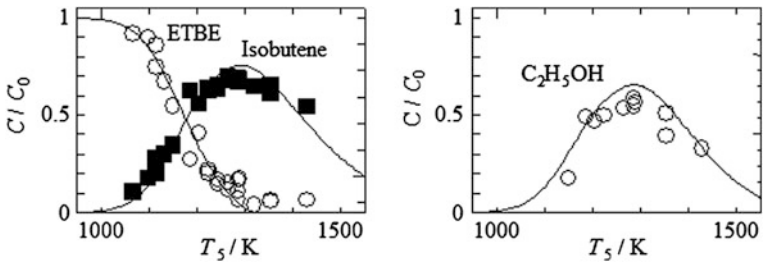

Fig. 6.4 Species concentration profiles for the pyrolysis of 3 % ETBE diluted in Ar at $P_5 = 1.9$–3.4 atm, effective heating time = 1.1–1.4 ms, *lines* simulation. C_0 denotes the initial concentration of ETBE, C those of ETBE and products as a result of shock heating

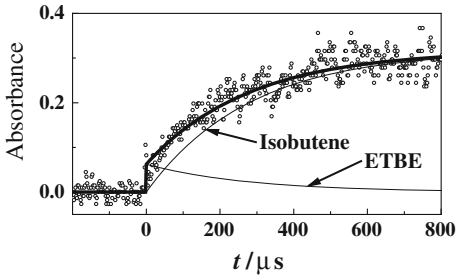

Fig. 6.5 A typical absorbance profile in ETBE pyrolysis at 195 nm; shock conditions, 0.0167 % ETBE diluted in Ar, $T_5 = 1{,}231$ K, $P_5 = 8.1$ atm

shown below, together with the Lambert–Beer law which relates concentrations and molar absorptivity:

$$\left[(CH_3)_3COC_2H_5\right] = \left[(CH_3)_3COC_2H_5\right]_0 \times \exp\{-(k_i + k_o)t\}$$
$$\left[(CH_3)_2C = CH_2\right] = k_i/(k_i + k_o)\left[(CH_3)_3COC_2H_5\right]_0 \times \exp[1 - \exp\{-(k_i + k_o)t\}],$$

where k_i and k_o signify the rate constants for the reaction producing isobutene and other products, respectively. The estimated rate constants (open circles), k_i, are shown in Fig. 6.6 together with the rate expression, 1.7×10^{14} exp(−254 kJ mol^{-1}/*RT*) s^{-1}, adopted to explain species concentration profiles. The rate expression estimated from species concentration profiles agrees well with those estimated by UV absorption spectroscopy.

6.2.4 Reactions of Oxygenates and Aromatic Hydrocarbons

The principle, data acquisition, and validation of single pulse shock tube are described above. The concentration profiles are more useful to examine reaction

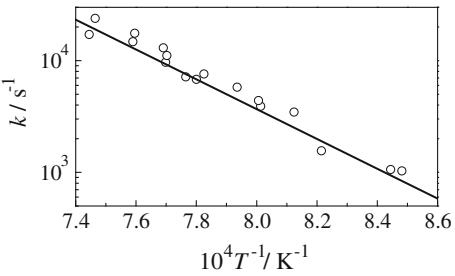

Fig. 6.6 Arrhenius plots for k_i; symbols are the rates estimated from UV absorption at 195 nm over pressure range between 2.5 and 8.9 atm, *line* is rate expression, 1.7×10^{14} exp $(-254.0$ kJ mol$^{-1}/RT)$ s^{-1} adopted to explain gas chromatographic results in single pulse shock tube

mechanisms because they reflect lots of information for reactions and their rate constants. Diethyl ether (DEE) (Yasunaga et al. 2010) mainly decomposes via unimolecular decomposition and hydrogen abstraction by radicals under shock tube conditions. Some of important reactions to explain the reactivity of DEE at high temperature are listed below:

$$C_2H_5OC_2H_5 \rightarrow C_2H_5OH + C_2H_4 \tag{6.2}$$

$$\rightarrow C_2H_5 + C_2H_5O \tag{6.3}$$

$$\rightarrow CH_3 + CH_2O\ C_2H_5 \tag{6.4}$$

$$C_2H_5OC_2H_5 + X \rightarrow CH_3CHOC_2H_5 + HX \tag{6.5}$$

$$\rightarrow CH_2CH_2OC_2H_5 + HX \tag{6.6}$$

where X indicates atoms and radicals like H, O, CH_3, and OH. Computer simulation can capture the observed concentration profile of C_2H_5OH when the rate constant of reaction (6.2) is described properly, because this is the sole reaction producing C_2H_5OH. Atoms and radicals abstract hydrogen atoms from DEE to produce $CH_3CHOC_2H_5$ and $CH_2CH_2OC_2H_5$. CH_3CHO and C_2H_5, C_2H_4 and C_2H_5O are produced from the uni-molecular decomposition of $CH_3CHOC_2H_5$ and $CH_2CH_2OC_2H_5$, respectively. The concentration of CH_3CHO includes the information about the rate of reaction (6.5), because $CH_3CHOC_2H_5$ is the principal producer of CH_3CHO. The concentration of DEE is sensitive to the total rate of DEE decomposition, which means that it has sensitivity to the five reactions listed above. As explained here, concentration profiles are so useful to examine the reaction mechanism that this method is applied to oxygenates and aromatic hydrocarbons whose reactivity are still unclear.

Polyaromatic hydrocarbons (PAH) are assumed as a soot precursor. Hydrogen abstraction/acetylene addition is a well-known (Bockhorn et al. 1983; Frenklach et al. 1985; Frenklach and Wang 1991; Wang and Frenklach 1997) mechanism of

the growth of PAH. The yields of acenaphthylene and naphthalene as a result of the reactions between naphthyl radicals and acetylene were measured in a single pulse shock tube (Lifshitz et al. 2009). The rate parameters estimated from ab-initio calculations explained these yields reasonably. Single pulse shock tube studies have also been conducted at high pressures, up to 50 bar, to investigate PAH formation and have revealed the importance of addition of cyclic radicals and molecules to molecular growth (Comandini and Brezinsky 2012).

The above examples demonstrate the use of single pulse shock tubes to investigate reactivity of oxygenates and mechanisms of PAH formation. However, they only scratch the surface of the detailed insights single pulse shock tube studies give to complex reaction mechanisms. With the very broad experimental range and ability to detect multiple species, single pulse shock tubes are a valuable tool to investigate fundamental chemical kinetic problems and provide comprehensive datasets for the development of complex mechanisms.

6.3 Time-of-Flight Mass Spectrometry and Shock Tubes

Time-of-flight mass spectrometry (TOF-MS) is a valuable although somewhat niche tool in shock tube research that leads to greater understanding of combustion mechanisms through 'real-time' measurement of gas composition and identification of products and intermediates. At the time of writing, there are three shock tube ST/TOF-MS apparatuses in routine use (Tranter et al. 2007; Dürrstein et al. 2011a, b) all of which are evolutions of the instrument of Bradley and Kistiakowsky (1961) which was developed in the early 1960s. Until his retirement in 2000, Kern (see Kern et al 2001 and references therein) produced the majority of ST/TOF-MS data related to combustion research including the important observation that recombination of propargyl radicals leads to the formation of benzene (Wu and Kern 1987); now considered one of the primary steps to the production of PAH in flames.

All current ST/TOF-MS experiments are conducted behind reflected shock waves and gases continually elute from the reaction zone via a small orifice (typically <0.3 mm) in the end-wall of the driven section into a chamber maintained at low pressure. Conditions are selected so that the eluting gases form a supersonic jet and the fast expansion rapidly cools the gases and quenches reactions thereby preserving the composition as it was in the shock heated reaction zone. The jet is directed into the ionization zone of the TOF-MS, with or without first being formed into a molecular beam with a skimmer, and a pulsed ionization source generates packets of ions that are mass analyzed providing time/concentration data. An example ST-TOF-MS interface is shown in Fig. 6.7.

Most ST/TOF-MS experiments are conducted at reflected shock pressures less than a few bar with the primary limitation being the need to keep a sufficiently low pressure, $<3 \times 10^{-5}$ Torr, in the ion source of the mass spectrometer while maintaining adequate signal levels. The experiments typically have an observation

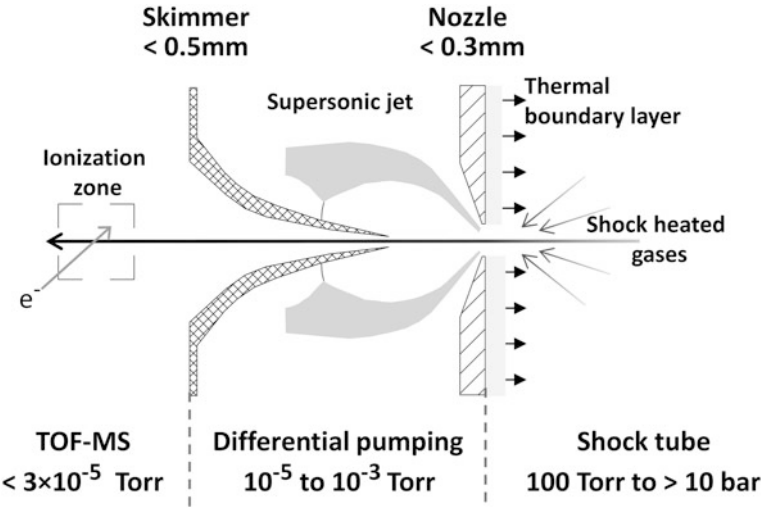

Fig. 6.7 Sketch of a differentially pumped interface between a shock tube and the ion source of a mass spectrometer. The mass spectrometer can be placed either on-axis with the shock tube or orthogonal to it. The skimmer may be removed and the nozzle moved to within 3 mm of the ionization zone

period of 1–2 ms during which mass spectra are acquired before the arrival of the shock wave and after reflection of the shock wave from the driven section end wall. To obtain adequate signal levels, the initial reagent concentrations are normally in the range 0.5–5 %.

All current ST/TOF-MS setups create ions with electron impact (EI) ionization sources which can be pulsed up to 150 kHz giving a mass spectrum every 6.67 μs. These sources can generally be tuned over a wide range of ionization energies although for ST/TOF-MS experiments they are typically not used below 28 eV due to insufficient signal intensity at lower energies. However, even at quite low energies EI ionization is rather brutal and tends to fragment molecules extensively making assignment of mass spectra challenging when multiple species are ionized simultaneously; a normal occurrence in ST/TOF-MS experiments. The complexity of spectra obtained is illustrated by experiments on the pyrolysis of ethylene glycol vinyl ether (EGVE), Fig. 6.8, where the fragments of EGVE also correspond to parent and fragment ions of many products and several products also share fragments. However, even for such complex spectra key mechanistic clues can be obtained (Yang et al. 2011).

Coupling a shock tube to a TOF-MS and obtaining reliable high quality data is not a trivial task and the challenges of building and running an early ST/TOF-MS are charmingly described by Moulton (1964). An excellent discussion of the ST/TOFMS technique is given in Kern et al. (2001) including details of calibration methods. A discussion of modern instruments with particular emphasis on sampling is available in Tranter et al. (2007) and a compact, adjustable interface between the shock tube and mass spectrometer is presented in Dürrstein et al. (2011b).

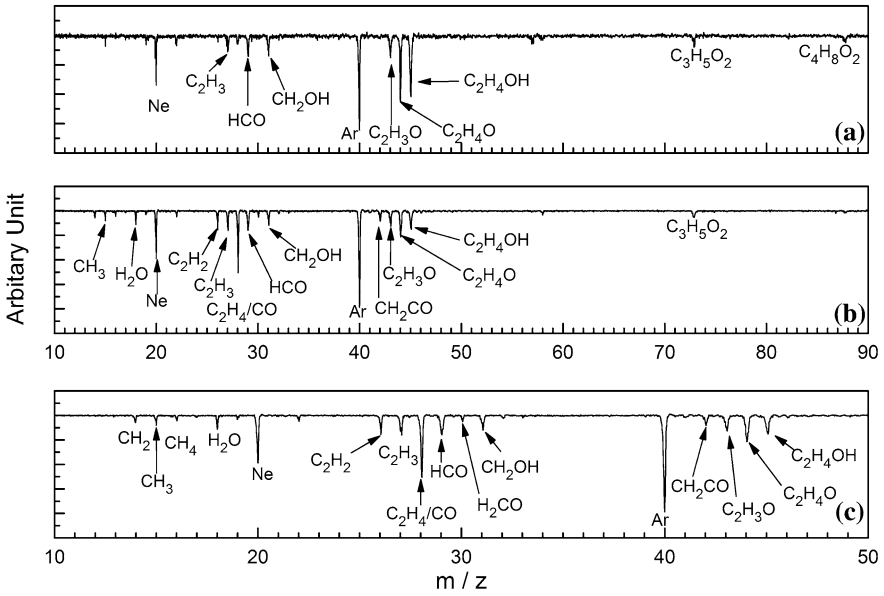

Fig. 6.8 Electron impact, 30 eV, mass spectra of the pyrolysis of ethylene glycol vinyl ether in a shock tube ($T_5 = 1{,}217$ K and $P_5 = 913$ Torr). Argon was added as an internal standard. **a** Pre-shock i.e. only EGVE, and the bath gas neon. **b** ~100 μs after reflection of the shock wave. **c** Expansion of a portion of **b**. Note that many possible products share the same fragments, e.g., H_2CO fragments to HCO in the ion source and HCO is also formed from fragmentation of EGVE. Reproduced by permission of the PCCP owner societies from Yang et al. (2011)

The above text broadly outlines the main features of ST/TOF-MS experiments but what may not be apparent is that these apparatuses incorporate many conflicting demands and a functioning ST/TOF-MS is the result of many compromises. Some of the main challenges related to effects of pressure and sampling are briefly discussed below although they are covered in detail in the above references.

The most obvious challenge is that the pressures in the shock tube are orders of magnitude greater than the operating pressures of a TOF-MS. One method of addressing this is to use a differentially pumped molecular beam sampling (MBS) interface such as shown schematically in Fig. 6.7. With this arrangement, less demands are placed on the vacuum pumps and relatively large, flat (~0.3 mm orifice) nozzles can be used with reflected shock pressures up to ~3–4 bar. As shown schematically in Fig. 6.7 a cold thermal boundary layer, TBL, is established following reflection of the shock wave and grows back into the shock heated zone. Gases from the shock heated zone are withdrawn through this layer. Voldner and Trass (1980) have shown that gases from the TBL are confined to the outer portion of the jet, at short times, and that the time taken for the TBL to engulf the sampled gases scales with the 4th power of the nozzle diameter. Thus, large diameter nozzles can significantly increase the sample time, and they are less susceptible to

blockage, a problem in pyrolytic studies. However, the orifice diameter must be sufficiently small that gases escaping through it do not create significant flow within the shock tube (Tranter et al. 2007). An additional advantage of the flat nozzle shown in Fig. 6.7 is that it is simple to manufacture. The benefits of a differentially pumped MBS have to be weighed against the two principal drawbacks. Firstly, signals can be weak particularly if the separation between the nozzle and skimmer is more than a few nozzle orifice diameters. Secondly, the nozzle and skimmer must be precisely aligned to ensure that only gases from the reaction zone in the shock tube are sampled and that none of the cold gases from the TBL enter the TOF-MS.

If the flat nozzle is replaced with a small conical nozzle, $\sim$1 mm high and 1 mm base diameter, then sampling from the TBL is avoided, at least for about 1 ms when the TBL becomes thick enough to engulf the nozzle. Such nozzles are relatively difficult to manufacture and spatial constraints make it difficult to obtain the optimum separation between nozzle and skimmer while maintaining good flow through the nozzle. A commonly used configuration with conical nozzles dispenses with the skimmer entirely. Here the advantage of differential pumping is lost and to prevent over pressurizing the TOF-MS the nozzle orifices are reduced, $<$0.1 mm. These smaller nozzles are more prone to blockage although judicious selection of reagents and concentrations can minimize this. If the nozzle is placed within 2–3 mm of the ionization source, then good signal levels can be obtained.

A further consideration is the orientation of the TOF-MS relative to the shock tube. In apparatuses that do not incorporate a skimmer they are normally co-axial which simplifies positioning the nozzle close to the ion source. However, both neutral species and ions will enter the TOF-MS requiring additional pumping capacity on the flight tube of the TOF-MS to maintain sufficiently low pressures in the vicinity of the detector ($<1 \times 10^{-6}$ Torr). If the TOF-MS is placed orthogonal to the flight tube then ions are extracted perpendicular to the path of the molecular beam and neutrals pass directly through the ion source and are evacuated from the chamber. With this arrangement maintaining good vacuum in the TOF-MS is simple but careful consideration has to be given to ion extraction to ensure efficient extraction. In the author's opinion, it is quite simple to build an apparatus that accommodates both arrangements and it is fairly easy to change the alignment of shock tube and TOF-MS to suit a particular experiment.

A final consideration of the effect of pressure in ST/TOF-MS experiments is that there is a large step change in pressure in the shock tube following reflection of the shock wave. Consequently, there is a corresponding increase in pressure in the ion source which results in the generation of more ions and stronger signals, Fig. 6.9. Thus, if one simply plots peak area, which is proportional to concentration, against reaction time meaningless kinetic data will be obtained. To compensate for the change in signal level with changing pressure a nonreactive standard, either the bath gas or often argon, is used to scale peak areas for each ionization/analysis cycle, see Kern et al. (2001) for details.

The following discussion focuses on the use of ST/TOF-MS experiments to investigate elementary reactions in the early stages of PAH formation. In

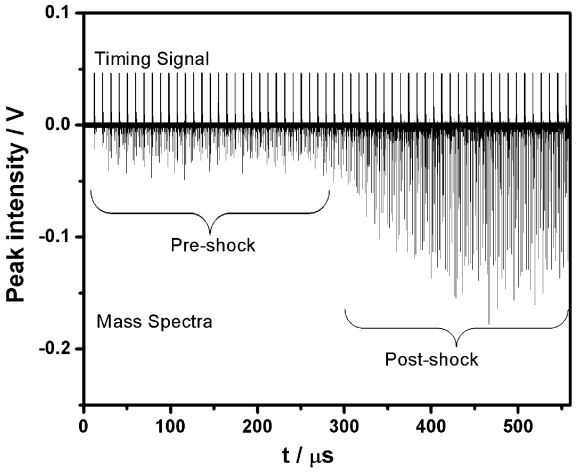

Fig. 6.9 ST/TOF-MS data obtained at an ionization cycle frequency of 105 kHz. $P_5 = 558$ Torr, $T_5 = 1{,}360$ K. The downward spikes, labeled as mass spectra, show the preshock as well as the postshock data. The upward spikes show the timing signals used to create ion packets in the molecular beam and extract them into the TOF-MS. Reprinted with permission from Tranter et al. (2007). Copyright 2007, American Institute of Physics

particular, the technique has proved most valuable in combination with other shock tube experiments such as laser schlieren densitometry and single pulse where complementary data are obtained. Often the experiments are also performed in conjunction with high level theoretical investigations to fully elucidate multi-channel reactions. Earlier in this chapter, the use of single pulse shock tubes to study PAH formation was briefly discussed. The following discussion illustrates the benefits of using multiple techniques to study complex problems such as PAH formation. For instance, the ST/TOFMS methods yield information about radical species and time histories that cannot be obtained by single pulse methods. But the single pulse methods provide mode details about stable species and over a broader experimental range than the ST/TOFMS can.

6.3.1 Formation of Polyaromatic Hydrocarbons

Determining reaction mechanisms for the formation of the building blocks of soot from small molecules and radicals in the gas phase has been an active topic of experimentalists and theoreticians. Currently, one of the main accepted mechanisms for formation of the first aromatic ring in flames is the association of two propargyl radicals followed by isomerization of the linear C_6H_6 molecules. This key step was first proposed by Kern (Wu and Kern 1987) from ST/TOF-MS experiments on allene dissociation. Although, later detailed theoretical studies (see

Miller and Klippenstein 2003 and references therein) revealed the complex sequence of isomerization steps that convert the linear adducts to benzene. In a combustion environment, a hydrogen atom can easily be abstracted from benzene by a number of radicals to give the phenyl, C_6H_5, radical, a key species in soot production. Phenyl radicals are quite stable and recombination could be competitive with other growth reactions such as addition of acetylene.

Earlier experimental studies considered biphenyl to be the sole product of phenyl self-reaction, (Heckmann et al. 1996). However, a mechanism based on this suggestion could not simulate shock tube/laser schlieren densitometry (ST/LS) experiments on phenyl self-reaction (Tranter et al. 2010). A weakness of the ST/LS technique is that it measures a global property, the density gradient, and one has to infer the chemistry through simulation of the data. ST/TOF-MS, however, directly identifies products and intermediates and complements the ST/LS experiments by providing key mechanistic information.

Results from ST/TOF-MS experiments on phenyl recombination with phenyl iodide as the precursor are shown in Fig. 6.10 and were a key part in understanding the complex nature of phenyl radical association. The upper panel shows a pre-shock mass spectrum of the reagent mixture containing phenyl iodide dilute in neon with a little argon as an internal standard, see Tranter et al. (2010) for details. The lower panel shows a mass spectrum from the reacting mixture. Clearly seen are *m/z* 154, biphenyl, and *m/z* 76 and 78, *o/m/p*-benzyne and benzene, respectively. The formation of *o/m/p*-benzyne simultaneously with benzene indicates that two phenyl radicals not only add to give biphenyl but also undergo

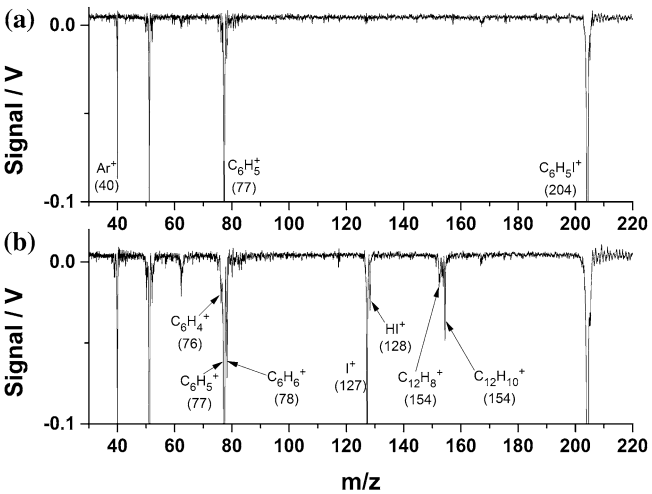

Fig. 6.10 TOF-MS from the dissociation of iodobenzene. Conditions: 2% C_6H_5I/3% Ar/95% Ne; $T_5 = 1{,}239$ K; $P_5 = 632$ Torr; ~250 μs after reflection of the shock wave. Reprinted (adapted) with permission from Tranter et al. (2010). Copyright 2010 American Chemical Society

disproportionation. While no attempt was made to extract kinetic data from the ST/TOFMS experiments, the mass spectra revealed new mechanistic paths which, when included in a model, provided good simulations of the ST/LS data. Furthermore, from the ST/LS results, rate coefficients and branching ratios for the recombination and dissociation reactions could be obtained, which were in excellent agreement with the theoretical predictions of Harding and Klippenstein (Tranter et al. 2010). It is particularly significant and surprising that at combustion temperatures the branching ratio (k_{dis}/k_{rec}) to *o/m*-benzyne is $\sim$0.5 suggesting that the role of benzyne radicals in PAH growth is much more significant than previously thought. Later, ST/TOF-MS studies (Dürrstein et al. 2011a) arrived at similar conclusions. Recently, single pulse shock tube experiments from Brezinsky's laboratory (Comandini et al. 2012) have confirmed the importance of *o*-benzyne in PAH growth.

Disproportionation/recombination should be quite general in association reactions of aromatic radicals and may also be a significant route for growth of halo-substituted aromatics. In Fig. 6.11 a mass spectrum from ST/TOF-MS experiments with perfluoroiodobenzene, C_6F_5I, is shown (Tranter 2013). These experiments are analogous to those with C_6H_5I and examine the self-reaction of perfluorinated phenyl radicals. The mass spectra in Figs. 6.10b and 6.11 are essentially identical apart from the increase in mass due to fluorine substitution. *o/m/p*-C_6F_4 radicals were not observed most likely because of low concentrations of these species. However, the peak at *m/z* 296, $C_{12}F_8$, can only come from recombination of two perfluorobenzyne radicals, compare. *m/z* 152 in Fig. 6.10b (Tranter et al. 2010).

A natural extension of the above experiments is to study dissociation and recombination of *o*-benzyne, the dominant C_6H_4 radical, by the ST/LS and ST/TOF-MS techniques (Tranter et al. 2012). For T > 2,000 K fluorobenzene dissociates by HF elimination, Fig. 6.12, in ST/LS experiments to give *o*-benzyne. These temperatures are also sufficient to dissociate *o*-benzyne radicals which primarily yield C_2H_2 and C_4H_2 (Zhang et al. 2007; Xu et al. 2007).

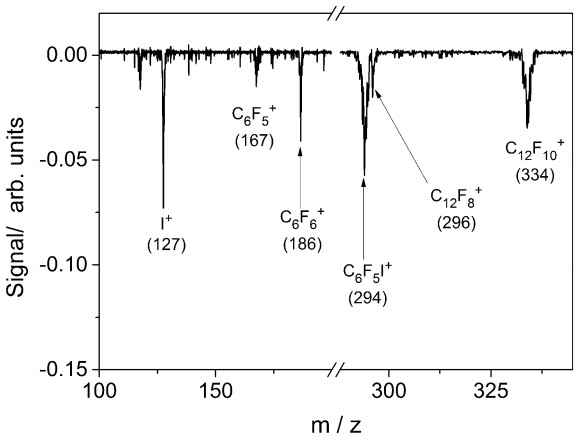

Fig. 6.11 TOF-MS from the dissociation of perfluoroiodobenzene. Conditions: 2% C_6F_5I/2% Ar/95% Ne; $T_5 = 1{,}639$ K; $P_5 = 734$ Torr; $\sim$200 μs after the reflection of the shock wave

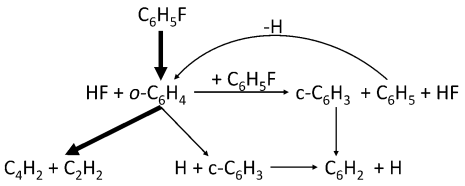

Fig. 6.12 Schematic for the dissociation of fluorobenzene at high temperatures

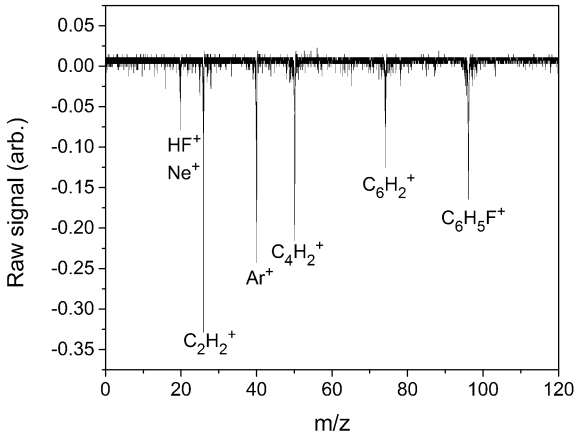

Fig. 6.13 TOF-MS from the dissociation of fluorobenzene. Conditions: 2 % C_6H_5F/3 % Ar/95 % Ne; $T_5 = 2{,}106$ K; $P_5 = 446$ Torr; 150 μs after the reflection of the shock wave

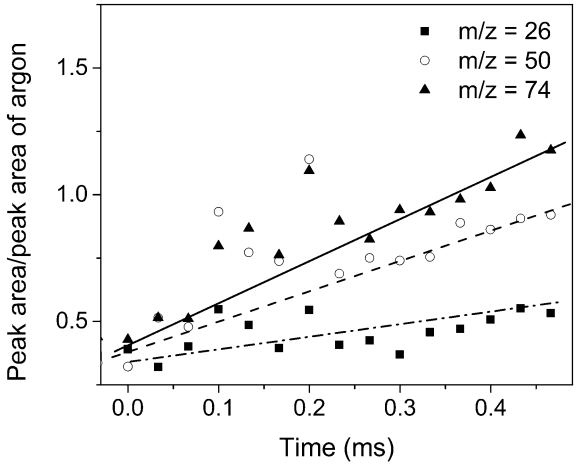

Fig. 6.14 Peak area (concentration)/time plots for the acetylenic species formed in the pyrolysis of fluorobenzene. Conditions as in Fig. 6.13. The scatter in the data is due to very low signal levels

Xu et al. (2007) also proposed a second, minor channel that leads to C_6H_2, triacetylene. ST/TOF-MS results from C_6H_5F experiments are shown in Figs. 6.13 and 6.14. The mass spectrum in Fig. 6.13 clearly shows peaks that can be attributed to acetylene, diacetylene and triacetylene. From Fig. 6.14, all three acetylenes appear to be formed simultaneously which is in apparent accord with the results of Xu et al. However, attempts to simulate the ST/LS experiments with a model based just on dissociation of *o*-benzyne failed mainly due to the relatively

slow dissociation of *o*-benzyne. Ultimately, it was concluded that *o*-benzyne is sufficiently stable that at lower temperature end of the ST/LS experiments it reacts preferentially with the parent molecule rather than decomposing, Fig. 6.12, providing an additional route to C_6H_2 molecules.

6.4 Conclusion

The methodology of using a single pulse shock tube with gas sampling is discussed. This simple method has been in use for more than a half century, and is still capable of producing useful speciation data for compounds undergoing pyrolysis and/or oxidation such as oxygenates and PAH.

This chapter also gives a brief overview of the benefit of ST/TOF-MS experiments and why they are worth pursuing despite the many challenges. It is the only technique that can measure all the hydrocarbon and oxygenate intermediates, products and radicals simultaneously in a shock tube experiment in real time. The current implementations of ST/TOF-MS with electron impact ionization are limited by fragmentation in the ion source although even when the fragmentation is severe useful mechanistic data can be obtained (Yang et al. 2011). Although kinetic data can be obtained from ST/TOF-MS experiments (Giri 2011; Giri et al. 2008), the real strength of the technique is identifying intermediates and their time evolution. Coupling a shock tube with selective photoionization by VUV radiation and MS is the next logical challenge for experimentalists.

Acknowledgments RST gratefully acknowledges support from the Office of Basic Energy Sciences, Division of Chemical Sciences, Geosciences, and Biosciences, U.S. Department of Energy, under contract number DE-AC02-06CH11357.

References

Bockhorn H, Fetting F, Wenz HW (1983) Investigation of the formation of high molecular hydrocarbons and soot in premixed hydrocarbon-oxygen flames. Ber Bunsen Ges Phys Chem 87:1067–1073

Bradley JN, Kistiakowsky GB (1961) Shock wave studies by mass spectrometry. I. Thermal decomposition of nitrous oxide. J Chem Phys 35:256–263

Comandini A, Brezinsky K (2012) Radical/pi-bond addition between o-Benzyne and cyclic C-5 hydrocarbons. J Phys Chem A 116:1183–1190

Davidson DF, Hong Z, Pilla GL et al (2011) Multi-species time-history measurements during n-dodecane oxidation behind reflected shock waves. Proc Combust Inst 33:151–157

Dürrstein SH, Olzmann M, Aguilera-Iparraguirre J et al (2011a) The phenyl+phenyl reaction as pathway to benzynes: an experimental and theoretical study. Chem Phys Lett 513:20–26

Dürrstein SH, Aghsaee M, Jerig L et al (2011b) A shock tube with a high-repetition-rate time-of-flight mass spectrometer for investigations of complex reaction systems. Rev Sci Instrum 82:084103

Frenklach M, Wang H (1991) Detailed modeling of soot particle nucleation and growth. Proc Combust Inst 23:1559–1566

Frenklach M, Clary DW, Gardiner WC et al (1985) Detailed kinetic modeling of soot formation in shock-tube pyrolysis of acetylene. Proc Combust Inst 20:887–901
Giri BR, Tranter RS (2007) Dissociation of 1,1,1-trifluoroethane behind reflected shock waves: shock tube/time-of-flight mass spectrometry experiments. J Phys Chem A 111:1585–1592
Giri BR, Kiefer JH, Xu H et al (2008) An experimental and theoretical high temperature kinetic study of the thermal unimolecular dissociation of fluoroethane. Phys Chem Chem Phys 10:6266–6273
Heckmann E, Hippler H, Troe J (1996) High temperature reactions and thermodynamic properties of phenyl radicals. Proc Combust Inst 26:543–550
Herzler J, Manion AJ, Tsang W (1997) Single-pulse shock tube studies of the decomposition of ethoxy compounds. J Phys Chem A 101:5494–5499
Hidaka Y, Shiba S, Takuma H, Suga M (1985) Thermal decomposition of ethane in shock waves. Int J Chem Kinet 17:441–453
Hidaka Y, Oki T, Kawano H, Higashihara T (1989) Thermal decomposition of methanol in shock waves. J Phys Chem 93:7134–7139
Kern RD, Singh HJ, Jhang Q (2001) Mass spectrometric methods for chemical kinetics in shock tubes. In: Ben-Dor G, Igra O, Lifshitz A (eds) Handbook of shock waves, vol 3. Academic Press, New York
Lifshitz A, Ben Hamou H (1983) Thermal reactions of cyclic ethers at high temperatures. I. Pyrolysis of ethylene oxide behind reflected shocks. J Phys Chem 87:1782–1787
Lifshitz A, Bauer SH, Resler EL (1963) Studies with a single pulse shock tube. The thermal cis → trans isomerization of 2-butene. J Chem Phys 38:2056–2063
Lifshitz A, Suslensky A, Tamburu C et al (2004) Thermal decomposition, isomerization and ring expansion in 2-methylindene. Single pulse shock tube and modeling study. J Phys Chem A 108:3430–3438
Lifshitz A, Tamaburu C, Dubnikova F (2009) Reactions of 1-naphtyl radicals with acetylene. Single-pulse shock tube experiments and quantum chemical calculations. Differences and similarities in the reaction with ethylene. J Phys Chem A 113:10446–10451
Miller JA, Klippenstein SJ (2003) The recombination of propargyl radicals and other reactions on a C6H6 potential. J Chem Phys A 39:7783–7799
Moulton DM (1964) Shock wave studies by time of flight mass spectrometry. Ph.D. thesis, Harvard University, Cambridge
Rajakumar B, Reddy KPJ, Arunan E (2002) Uni-molecular HCl elimination from 1,2-dichloethane. J Phys Chem A 106:8366–8373
Simmie JM (2003) Detailed chemical kinetic models for the combustion of hydrocarbon fuels Prog. Energy Combust Sci 29:599–634
Simmie JM, Quiring WJ, Tschuikow-Roux E (1969) The thermal decomposition of perfluoro-cyclobutane in a single-pulse shock tube. J Phys Chem 73:3830–3833
Sivaramakrishnan R, Tranter RS, Brezinsky K (2006) High pressure pyrolysis of toluene. 1. Experiments and modeling of toluene decomposition. J Phys Chem A 110:9388–9399
Tranter RS (2013) unpublished work
Tranter RS, Giri BR, Kiefer JH (2007) Shock tube/time-of-flight mass spectrometer for high temperature kinetic studies. Rev Sci Instrum 78:034101
Tranter RS, Klippenstein SJ, Harding LB et al (2010) Experimental and theoretical investigation of the self-reaction of phenyl radicals. J Phys Chem A 114:8240–8261
Tranter RS, Lynch PT, Annesley CJ (2012) High temperautre sources of phenyl and benzyne radicals. 22nd international symposium Gas Kinet. University of Colorado at Boulder, Boulder, CO, 18–22 June 2012
Tsang W, Lifshitz A (1999) Kinetic stability of 1,1,1-trifluoroethane. Int J Chem Kinet 30:621–628
Tsang W, Lifshitz A (2001) Single pulse shock tube. In: Ben-Dor G, Igra O, Lifshitz A (eds) Handbook of shock waves, vol 3. Academic Press, New York
Voldner EC, Trass O (1980) Evaluation of thermal-boundary layer interaction in shock-tube sampling for kinetic-studies J Chem Phys 73:1601–1611

Wang H, Frenklach M (1997) A detailed kinetic modeling study of aromatics formation in laminar premixed acetylene and ethylene flames. Combust Flame 110:173–221

Wu CH, Kern RD (1987) Shock tube study of allene pyrolysis. J Phys Chem 91:6291–6296

Xu C, Braun-Unkhoff M, Naumann C et al (2007) A shock tube investigation of H atom production from the thermal dissociation of ortho-benzyne radicals Proc. Combust Inst 31:231–239

Yang X, Kiefer JH, Tranter RS (2011) Thermal dissociation of ethylene glycol vinyl ether. Phys Chem Chem Phys 48:21288–21300

Yasunaga K, Kuraguchi Y, Hidaka Y et al (2008) Kinetic and modeling studies on ETBE pyrolysis behind reflected shock waves. Chem Phys Lett 451:192–197

Yasunaga K, Gillespie F, Simmie JM et al (2010) A multiple shock tube and chemical kinetic modeling study of diethyl ether pyrolysis. J Phys Chem A 114:9098–9109

Yasunaga K, Mikajiri T, Sarathy M et al (2012) A shock tube and chemical kinetic modeling study of the pyrolysis and oxidation of butanols. Combust Flame 159:2009–2027

Zhang X, Maccarone AT, Nimlos MR et al (2007) Unimolecular thermal fragmentation of ortho-benzyne J. Chem Phys 126:44312